FAD-binding site and NAD(P) reactivity in human renalase, a new enzyme involved in blood pressure regulation

Mario Milani[1,2], Francesco Ciriello[1], Sara Baroni[1], Vittorio Pandini[1], Giulia Canevari[1,3], Martino Bolognesi[1,2], Alessandro Aliverti[1*]

[1]Dipartimento di Scienze Biomolecolari e Biotecnologie, Università degli Studi di Milano, via Celoria 26, 20133 Milano, Italy.

[2]CNR-Istituto di Biofisica, Università degli Studi di Milano, via Celoria 26, 20133 Milano, Italy.

[3]Department of Chemical Core Technologies, Nerviano Medical Sciences, Oncology, Viale Pasteur 10, Nerviano 20014, Italy.

*Correspondence to: Alessandro Aliverti, Dipartimento di Scienze Biomolecolari e Biotecnologie, Università degli Studi di Milano, via Celoria 26, 20133 Milano; phone: +39 02 50314897; fax: +39 02 50314895; e-mail: alessandro.aliverti@unimi.it

Running title: Crystal structure of human renalase

Summary

Renalase is a recently discovered flavoprotein that regulates blood pressure, sodium and phosphate excretion, and has a cardioprotectant action through a mechanism that is scarcely understood to date. It has been proposed to act as a catecholamine-degrading enzyme, either via O_2- or NADH-dependent mechanisms. Here we report the renalase crystal structure at 2.5 Å resolution together with new data on its interaction with nicotinamide dinucleotides. Renalase adopts the *p*-hydroxybenzoate hydroxylase fold topology, comprising a Rossmann fold based FAD-binding domain, and a putative substrate-binding domain, containing a five-stranded antiparallel β-sheet. A large cavity (228 $Å^3$), facing the flavin ring, presumably represents the active site. Compared to mono- or poly-amine oxidases, the renalase active-site is fully solvent exposed and lacks the 'aromatic cage' for binding the substrate amino-group. Renalase has extremely low diaphorase activity, displaying lower k_{cat} but higher k_{cat}/K_m for NADH compared to NADPH. Moreover, its FAD prosthetic group becomes slowly reduced when it is incubated with NAD(P)H under anaerobiosis, and binds NAD^+ or $NADP^+$ with K_d values of *ca.* 2 mM. The absence of a recognizable NAD(P)-binding site in the protein structure and its poor affinity/reactivity towards NAD(H) and NADP(H) suggest that these are not physiological ligands of renalase. Although our study does not answer the question of what the catalytic activity of renalase is, it provides a firm framework for testing hypotheses on the molecular mechanism of its action.

Keywords: chronic kidney disease, end-stage renal disease, hypertension, phosphate excretion, flavoprotein structure.

Abbreviations

MAO, monoamine oxidase; INT, 2-(4-iodophenyl)-3-(4-nitrophenyl)-5-phenyltetrazolium chloride; WST1, 2-(4-iodophenyl)-3-(4-nitrophenyl)-5-(2,4-disulfophenyl)-2H-tetrazolium sodium salt; HT, hydride transfer; rmsds, pairwise root-mean-square deviations; PHBH, *p*-hydroxybenzoate hydroxylase; DAAO, D-ammino acid oxidase; PAO, polyamine oxidase; MR, molecular replacement.

Introduction

Renalase was identified in 2005 in a study focused on new links between chronic kidney diseases and their cardiovascular complications.[1] The human renalase gene (*RNLS*) is located on chromosome 10 and includes 10 exons.[2] Various isoforms arising from alternative splicing have been reported, two of which (renalase1 and renalase2) are annotated in genome databases (GenBank accession nos. **NP_001026879** and **NP_060833**, respectively). *RNLS* is expressed in kidneys, heart, skeletal muscle, brain and small intestine;[3] the main product (renalase1) has been detected also in blood plasma and urine.[2] End-stage renal disease is associated to lowered plasma renalase1 levels, indicating that kidneys are the source of the circulating protein.[1] Renalase has also been proposed as an early biomarker of acute kidney ischemia.[4] Intravenous administration of renalase1 was found to decrease blood pressure and heart rate in normal rats,[1] while its subcutaneous injection had an intense and prolonged antihypertensive effect in an animal model of salt-sensitive hypertension,[4,5] and its perfusion was found to play a heart protective effect in a cardiac ischemia mouse model.[2] Furthermore, *RNLS* gene inactivation in mouse resulted in an increased sympathetic activity, tachycardia and hypertension.[6] Two allelic variants of renalase, displaying similar frequencies in the human population, carrying Glu or Asp at position 37, are known. The Asp variant was found to correlate significantly with an increased risk of developing essential hypertension and cardiac syndromes.[7,8] It has been proposed that renalase could modulate the intrarenal dopamine system, affecting sodium and phosphate excretion.[4,5,9] In a rat model of chronic heart failure, the lowered blood renal flow is associated to a decrease in kidney renalase synthesis and norepinephrine clearance.[10]

Despite its potential impact on treatment of some of the "big killer" diseases in the developed world, an understanding of renalase action at the molecular level has not been reached yet. Stemming from its sequence similarity to flavin-dependent monoamine oxidases

(MAOs), it has been suggested that renalase could be a catecholamine-degrading flavoenzyme.[1,11,12] Evidence has been provided for two possible catalytic mechanisms: O_2-dependent direct oxidation of the amine substrate (as in the case of MAOs), or its NADH-dependent degradation, mediated by superoxide radical generation.[8] However, the turnover rate of renalase seems too low to fully justify its physiological effects; moreover, the actual presence of a catecholamine-degrading activity in blood plasma, other than that supported by semicarbazide-sensitive amine oxidase, has been excluded by some authors.[13] For two recent comprehensive reviews on renalase, the reader is referred to Refs. 4 and 14. Renalase is highly conserved in mammals, but orthologs are present in protists (*Phytophthora infestans* T30-4; 27% sequence identity), cyanobacteria (*Cyanothece* sp.; 28% identity), and bacteria (*Spirosoma linguale*; 26% identity), suggesting different biological functions associated with similar fold and possibly similar catalyzed reaction (*see* Fig. 5A).

With the aim of elucidating its catalytic mechanism, we produced an *in vivo* folded form of human renalase1 in *Escherichia coli*.[15] The recombinant protein was found to contain non-covalently bound FAD, thus providing the first direct evidence that it is a flavoprotein. Here we present a further step towards the elucidation of its structure-function relationships, reporting its three-dimensional structure solved at 2.5 Å resolution. These data, together with kinetic and nucleotide-binding studies, provide new hints on the active-site structural organization in this intriguing enzyme.

Results

Redox properties and reactivity of the renalase FAD prosthetic group

Since here we report solely on the properties of human renalase1, we use the term "renalase" throughout this paper to indicate this specific isoform, unless otherwise stated. To shed light onto renalase enzymatic activity, we investigated the stability and protonation state of the semiquinone form of its FAD cofactor, which are important criteria for flavoprotein classification.[16,17] Anaerobic renalase solutions were subjected to stepwise photoreduction at different pH values, and the resulting absorption spectra recorded. As shown in Fig. 1, the bound FAD could be readily reduced by the light/EDTA/deazariboflavin system, and was reoxidized to yield the original spectrum when the solution was exposed to air. More interestingly, at acidic pH, a significant amount of a species displaying a broad absorption band in the 550-650 nm region, identifiable as neutral flavin semiquinone, was formed during reduction. Above pH 7, the FAD blue semiquinone was undetectable (Fig. 1, inset), without clear evidence of accumulation of its red anionic form. This behavior is at variance from what is observed for both MAO-A and MAO-B, as well as for their homolog from *Aspergillus niger* (MAO-N, containing a noncovalently-bound FAD), which strongly stabilize the FAD anionic semiquinone.[18,19]

FAD reactivity with sulfite is a distinct key criterion for flavoenzyme classification, since a high stability of the sulfite-isoalloxazine adduct usually correlates with a high O_2-reactivity.[20] Renalase was found to react with sodium sulfite yielding a complex with a K_d of 1.8 ± 0.2 mM (Fig. 2). The reaction was found to be very slow, with constants for complex formation and dissociation of 0.056 ± 0.007 min^{-1} and 0.025 ± 0.003 $min^{-1}mM^{-1}$, respectively. Again, these results suggest both that renalase is not a typical oxidase, and that it differs dramatically from MAOs, which do not react at all with sulfite due to hydrophobicity of their active sites.[21]

Reactivity of renalase with nicotinamide dinucleotides

Renalase has been reported to catalyze slow O_2 reduction in the presence of NADH yielding the superoxide radical.[8] Since such NADH oxidase reaction suggests the possibility that renalase could be either a dehydrogenase or a monooxygenase, we studied in detail its NAD(P)H-dependent diaphorase activities using various artificial electron acceptors, such as 2-(4-iodophenyl)-3-(4-nitrophenyl)-5-phenyl-2*H*-tetrazolium chloride (INT), 2-(4-iodophenyl)-3-(4-nitrophenyl)-5-(2,4-disulfophenyl)-2H-tetrazolium sodium salt (WST1) and $K_3Fe(CN)_6$. The recombinant form of renalase we have previously produced in *E. coli*[15] corresponds to its Asp37 variant. Since this variant has been reported to possess a lower catalytic activity than the Glu37 form,[8] we have introduced the Asp37Glu replacement in the protein by site-directed mutagenesis. The two variants of renalase displayed indistinguishable catalytic properties *in vitro*. As the Asp37 variant yielded crystals suitable for X-ray analysis, here we focus on the properties of this form.

Renalase displayed a low but measurable catalytic activity only *vs.* INT and WST1, the former substrate being the preferred one. Plots of the steady-state kinetic data for the INT-reductase reactions are shown in Fig. 3. The steady-state kinetic parameters (Table 1) show that renalase is slightly but significantly more specific for NADH rather than NADPH, although it displays a higher k_{cat} value with the latter cosubstrate. The reductive half-reaction of the catalytic cycle, *i.e.* the reduction of protein-bound FAD by NAD(P)H, was investigated under anaerobic conditions. Both nucleotides were able to transfer reducing equivalents to the renalase prosthetic group. Apparent first-order rate constants (k_{red}) for hydride transfer (HT) of $1.5\times10^{-2} \pm 2\times10^{-4}$ min^{-1} and $2.7\times10^{-2} \pm 1\times10^{-4}$ min^{-1}, were obtained for 1 mM NADH (k_{red}^{NADH}) and NADPH (k_{red}^{NADPH}), respectively.

In order to further investigate the interaction of the protein with nicotinamide dinucleotides, spectrophotometric titrations of renalase with $NAD(P)^+$ were performed. As shown in Fig. 4, renalase clearly interacts with both dinucleotides, forming complexes whose remarkably strong difference absorption spectra are very similar. Titrations follow the theoretical curve expected for a 1:1 stoichiometry (Fig. 4, inset). The K_d of the complexes of renalase with NAD^+ and $NADP^+$ were 2.2 ± 0.1 mM and 1.6 ± 0.1 mM, respectively. Interestingly, 2'-P-AMP titration yielded a similar K_d value (1.2 ± 0.3 mM), but a far less intense difference spectrum (Fig. 4), implying that the adenylate portion of $NADP^+$ provide most of the binding energy, while the nicotinamide moiety plays a main role in the perturbation the isoalloxazine environment. However, titration of renalase with up to 6 mM 5'-AMP did not result in any spectral change, suggesting that a single phosphate group in the ligand is not sufficient to provide enough binding energy and/or the ability to perturb isoalloxazine upon binding.

Renalase crystal structure

The crystal structure of renalase was solved through a composite molecular replacement approach, and refined at 2.5 Å resolution (Rgen /Rfree = 21.7/26.0%; see Table 2); two renalase molecules are hosted per asymmetric unit. The two independent molecules (A and B) display very similar overall conformations, with a pairwise root-mean-square deviations (rmsds) of 0.41 Å calculated over 330 Cα pairs. A contained contact region (467 $Å^2$) is observed between the two molecules, in keeping with the monomeric character of renalase in solution, shown by previous gel filtration and dynamic light scattering studies.[15] The refined electron density allowed us to model all the protein amino acids, with the exception of a few that are localized in the substrate-binding domain: *i.e.* Ser25 (chain A), Lys99-Glu100 (A, B), Asp140 (B), Ser150 (B), Glu201 (B), Lys205-Ile206 (A), Ser236 (B)-

Glu237 (A, B), Cys300 (B).

The renalase molecule displays a bean-like elongated shape with the longer axis of about 60 Å and the shorter of 35 Å. The two lobes of the bean host respectively the FAD-binding domain (amino acids 1-42, 109-189, 294-341; Fig 5B, red) and the putative substrate-binding domain (43-108, 190-294; Fig 5B, blue and green). The two domains are bent forming a wide and deep cleft at the center of the protein that, like a belt, runs perpendicularly to the protein longest axis. Such crevice (positively charged) crosses the protein surface opposite to the partially exposed isoalloxazine ring. The FAD molecule is buried within the protein except for part of the isoalloxazine ring (see below), a small portion of the adenine ring, and part of the adenosine ribose near the pyrophosphate bridge (located next to the mentioned cleft). The FAD-binding domain architecture is based on a Rossman fold (as in the glutathione reductase family),[22] composed of a six-stranded central β-sheet (with β3β2β1β4β6β5 topology), surrounded by six α-helices, and by an additional three-stranded mixed β-sheet. The putative substrate-binding domain consists of an antiparallel five-stranded β-sheet surrounded by three α-helices and by one β-hairpin. Moreover, it includes a small subdomain (amino acids 62-108), projecting helix α3 toward the FAD-binding domain (Fig. 5B, green).

The general fold of renalase classifies it as a member of the flavoprotein superfamily sharing the *p*-hydroxybenzoate hydroxylase (PHBH) fold topology, which includes both oxidase and non-oxidase enzymes.[23] Most PHBH-like enzymes catalyzing the oxidation of amines belong to one of two possible structural groups: the MAO and the D-amino acid oxidase (DAAO) families.[24] Renalase is structurally more similar to the MAO-like than to DAAO-like enzymes. A search performed through the DALI server (http://ekhidna.biocenter.helsinki.fi/dali_server/) for proteins structurally homologous to renalase yielded a putative protoporphyrinogen oxidase (PDB ID: **3LOV**, Z-score 28.9,

residue identity 19%), in addition to L-amino acid oxidase, a Lys-specific histone demethylase, and an amine oxidase (PDB IDs 2JB2, 2UXX, and 2BXR, respectively).

With the exception of histone demethylase, the main feature common to all the protein structures highlighted by DALI as structurally similar to renalase is the presence of an additional stretch of 110-140 amino acids that is entirely absent in renalase (Fig. 6A, left). This structural element corresponds to an additional domain that would be inserted between strands β7 and β8 of renalase substrate-binding domain. Multiple alignment shows that the regions flanking such 'missing' domain are not conserved (Fig. 5A). Interestingly, one of the short segments disordered in the renalase crystal structure corresponds exactly to the insertion point of the 'missing' domain (Lys99-Glu100). The functional roles played by this domain in the renalase homologs are markedly different: in protoporphyrinogen oxidase it is a membrane-binding domain, while in L-amino acid oxidase it is a helical domain responsible for protein dimerization. On the contrary, in MAOs and polyamine oxidase (PAO) it is an integral part of the substrate-binding domain.

FAD binding

Nineteen residues are directly involved in FAD binding, six of which establish electrostatic or polar interactions with the cofactor (Fig. 6B). Only two of the latter interactions involve side chain atoms (conserved residues Thr12 and Arg42 linked to the FAD pyrophosphate), the others being due to main chain atoms. Access to the dimethylbenzene moiety of the isoalloxazine ring is blocked by the conserved Trp288, while the cofactor pyrimidine ring is quite solvent exposed (Fig. 6A, right), establishing hydrogen bonds with the main chain atoms of Tyr62 and Phe324 and displaying van der Waals interactions with Ala59.

Putative substrate-binding site

The absence of the 'missing' domain in renalase (see above) results in the presence of a wide surface concavity that is the entry site for the enzyme main core cavity, where the FAD cofactor is hosted (Fig. 6A, right). As a consequence, the putative enzyme active site is solvent exposed, as underscored by the presence of five water molecules above the isoalloxazine ring. The active site cavity has a volume of about 224 $Å^3$ and can be roughly divided into two hemispheres, one composed of aromatic residues, the other of polar residues, centered on the isoalloxazine ring. The aromatic hemisphere (roughly above the isoalloxazine pyrimidine ring) is characterized by residues Tyr62 (mostly conserved), Tyr214 and Phe223 (aromaticity conserved), the two Tyr residues being mutually hydrogen-bonded (2.7±0.2 Å; mean of the two subunits). The polar hemisphere is lined by Gln292, Arg193, His245 (mostly conserved) and Arg222, and displays an overall positive charge (Fig. 6B). The water molecules found in the cavity bridge between the two sides but their locations are not conserved in the two renalase chains, suggesting that the site is suited to accommodate polar compounds. A sulphate anion, hydrogen-bonded to Thr247, and electrostatically compensated by Arg193 and Arg222, is present in both asymmetric unit renalase molecules, at the external border of the polar cavity (Fig. 6B). Since renalase has been proposed to represent a new form of MAO,[1,11] a structural comparison with the active site of the latter enzyme is useful. The overlay of the three-dimensional structure of renalase with those of MAO A, MAO B and PAO led to the observation that the position of the active-site cavity is highly conserved in all these enzymes. However, residues critical for catalysis of amine oxidation are not maintained in renalase. In particular, Lys296 (MAO B numbering), is replaced by His245, and the so-called 'aromatic cage' (formed by Tyr398 and Tyr435 in MAO B)[25,26] is absent in renalase, where the two aromatic residues are replaced by Gln292 and Asn323 (Fig. 6B).

Discussion

The functional part of the study on renalase here described had two main purposes: (i) assessing the prosthetic group key chemical features that allow flavoprotein classification, and (ii) analyzing the interaction of renalase with nicotinamide dinucleotides, as conceivable cosubstrates of the enzyme. Concerning the first question, here we show that renalase provides a mild stabilization of the neutral form of the flavin semiquinone and that the renalase-bound FAD forms a sulfite-adduct, although slowly and with low affinity. Both features do not classify renalase as a MAO-like enzyme. Moreover, lack of stabilization for the FAD anionic semiquinone, and the previous observation that renalase reacts with O_2 producing the superoxide anion rather than hydrogen peroxide,[8] indicate that renalase is probably not even an oxidase.

As far as the second question is concerned, we confirm that renalase catalyzes NAD(P)H-dependent diaphorase reactions, as recently reported by others.[8] In addition, we provide evidence for direct HT from NAD(P)H to the enzyme, and for 1:1 complex formation with the oxidized dinucleotides and a NADP analog. However, the exceedingly low k_{cat} and k_{cat}/K_m values observed in the steady state reactions, confirmed by very slow HT in the reductive half reaction and millimolar affinity of the enzyme for $NAD(P)^+$, strongly suggest that NADH and NADPH are not renalase physiological substrates. Such conclusion is in line with the absence of an evident NAD(P)-binding site in the enzyme three-dimensional structure. Since PHBH, which shares the same general fold of renalase, is known to bind NADPH (unconventionally) at the protein surface in a groove crossing the FAD cavity,[27,28] we employed molecular modeling, to assess whether renalase could accommodate NADPH in a similar way. Our structural comparisons indicate that FAD is much more deeply buried inside renalase than inside PHBH, making the putative NADPH-binding site sterically

blocked in renalase. Thus, whereas NADPH can access the FAD isoalloxazine ring of PHBH with limited conformation changes, a similar NADPH binding mode would appear catalytically unproductive in renalase. To explain the slow reactivity of renalase towards NAD(P)H, we speculated that nicotinamide dinucleotides might access FAD through the putative substrate-binding cavity.

A further point that needs to be discussed is the recent report that the Glu37 allelic variant of the protein displays higher catalytic efficiency (k_{cat}/K_m^{NADH}) in the reductase reaction, relative to the Asp37 form.[8] The crystal structure of the protein here described shows that residue 37 is located in a surface loop at the interface between the two domains, far from the active site. Moreover, consistent with structural evidences, we found no difference between the diaphorase activity of the two allelic variants of the enzyme. This discrepancy could be ascribed to the fact that we isolated renalase forms that underwent folding and FAD incorporation within *E. coli* cells,[15] while catalytic differences between variants were detected on proteins that were refolded *in vitro*.[8] Indeed, it has been shown that *in vitro* refolding may results in significant alterations of the properties of flavoproteins.[29]

In conclusion, the structural data firstly here reported are in keeping with the results of our previous and current functional studies pointing out that renalase is not a MAO and most probably not an oxidase. On the other hand, structural comparisons of renalase with its homologs do not allow to shed additional light on the reaction catalyzed by this enzyme. Taken together, our observations suggest that the substrate of renalase may be a large polar molecule, possibly carrying a negative charge; the chemical process catalyzed by renalase on such substrate would be different from an oxidase reaction.

Materials and Methods

NAD^+, $NADP^+$, NADH, NADPH, 2'-phospho-AMP, 5'-AMP, INT and WST1 were purchased from Sigma-Aldrich.

Renalase expression and purification

The variant of human renalase carrying Asp at position 37 was produced in the Rosetta(DE3) *E. coli* strain, transformed with the pET-SUMO-RNLS.[15] To obtain the other known widespread variant of the protein,[8] a point mutation resulting in the Asp37Glu substitution was introduced in the renalase coding sequence of the above plasmid, using the QuikChange® Lightning Site-Directed Mutagenesis Kit (Stratagene), in conjunction with the complementary oligonucleotides 5'-GGGACAAGGCTGAGGACTCAGGGGGAAG-3' and 5'-CTTCCCCCTGAGTCCTCAGCCTTGTCCC-3 (base changes underlined). Both recombinant forms of renalase were produced and purified according to the procedure previously reported.[15] Renalase concentration was quantified on the basis of the extinction coefficient of 11.3 $mM^{-1}cm^{-1}$ at 457 nm.[15]

Photoreduction experiments, ligand-binding studies and activity assays

All spectrophotometric measurements were performed either on a 8453 diode-array (Agilent) or a Cary 100 double-beam (Varian) spectrophotometer. Anaerobic stepwise photoreduction of the renalase FAD prosthetic group was carried out using the light/EDTA system.[30] Samples of *ca*. 15 μM renalase in 10 mM phosphate-NaOH/10 mM pyrophosphate-NaOH, at pH values ranging from 5.5 to 9.5, containing 15 mM EDTA and *ca*. 1.5 μM deaza-riboflavin, were brought to anaerobic conditions in a sealed cuvette by successive cycles of N_2 flushing and application of vacuum. Spectra were recorded before and as after successive illumination periods, until full reduction was obtained in a total irradiation time of about 4

min. Sodium sulfite titration of renalase was performed in PBS at 25 °C. Spectra were recorded before and after successive additions of allowing the reaction to reach equilibrium after each increase in ligand concentration. From the time course of the spectral change accompanying adduct formation, the pseudo-first order rate constants of the process were obtained at different Na_2SO_3 concentrations. The secondary plot of this apparent constant as a function of ligand concentration yielded the individual constants for adduct formation and dissociation from the slope and the intercept of the plot, respectively. The putative reductive half-reaction catalyzed by renalase, *i.e.* the HT from NAD(P)H to FAD was monitored spectrophotometrically at 37 °C, by recording the spectra of anaerobic solutions of 5 μM renalase in 50 mM Tris-HCl, pH 7.2, at various reaction times after the addition of NADH or NADPH at different concentrations. Spectrophotometric active-site titrations of renalase with $NADP^+$, NAD^+, 2'-P-AMP, or 5'-AMP were carried out at 25 °C in 50 mM Tris-HCl, pH 7.4, according to the procedure described elsewhere.[31] NADH- and NADPH-dependent diaphorase activities of renalase were assayed at 37 °C in 50 mM Tris-HCl, pH 7.2, using a fixed concentration of either 100 μM INT or 500 μM WST1 as electron acceptors. The reaction mixture included 2.6 μM renalase and a variable concentration of reduced dinucleotide in the range 0.05-2 mM. In the case of the INT-dependent reaction, 0.1% triton X-100 was also included to avoid precipitation of the formazan product. The time-course of the absorbance increase at the appropriate wavelength was monitored continuously and steady-state rates were calculated using the extinction coefficient of 18.5 $mM^{-1}cm^{-1}$ at 490 nm and 37 $mM^{-1}cm^{-1}$ at 450 nm for INT and WST1, respectively.

Crystallization and structure solution

Renalase crystals were obtained in sitting drop set-up, mixing 0.2 μl of protein, (c = 24 mg/ml; supplemented with freshly added 10 mM DDT) and 0.1 μl of reservoir solution (30%

PEG 8k, 0.1 M sodium cacodylate, pH 6.5, 0.2 M ammonium sulphate). Small crystals grown in about five days at 20 °C, with average dimension of 50×25×25 μm^3. Crystals were transferred to a cryoprotectant solution (32% PEG 8k, 0.1 M sodium cacodylate, pH 6.5, 0.2 M ammonium sulphate, 25% glycerol) before to be flash cooled in liquid nitrogen. Diffraction data were collected at ESRF beam line id23-2. The crystal, belonging to the monoclinic space group $P2_1$, diffracted at 2.5 Å resolution. During data collection the crystal suffered of radiation damage causing a reduced completeness of data (84.7%). While the color of crystals used for data collection indicated that bound FAD was unequivocally oxidized, minor/partial reduction of the coenzyme during X-ray irradiation cannot be excluded. The final model was of no help in revealing the oxidation state of the cofactor, since the two nitrogen atoms of FAD were found not involved in hydrogen bonds. Renalase structure was solved by molecular replacement (MR; program 'Molrep')[32]. The model used for MR search was built starting from the atomic coordinates of the q888a4 oxidoreductase of *Pseudomonas syringae* (a FAD-containing protein of unknown function; PDB ID: **3KKJ**), divided into two domains: the FAD binding domain (Mod1, amino acids 2-33, 124-181, 278-329) and the cofactor binding domain (Mod2, amino acids 82-99, 185-275), including about 74% of the renalase residues. Since Matthews analysis suggested the presence of two molecules in the crystal asymmetric unit (solvent content 57%), MR search (max resolution 3.5 Å) was performed in two subsequent steps: first to locate two copies of Mod1 (Rfac/Scor = 0.572/0.445) and then the remaining two copies of Mod2 (Rfac/Scor = 0.568/0.465). After rigid body refinement (R/Rfree 0.522/0.514) and constrained refinement (R/Rfree 0.435/0.488; 'Refmac')[33] we started mutating amino acids and manual rebuilding ('Coot')[34]. A clear electron density was present in the FAD binding site and the ligand model was therefore built. The programs 'Parrot'[35] and 'Buccaneer' were used to help modelling during the manual (re)building procedures, omit maps were produced to correct for errors in the

model, and programs ‘Refmac5’ and ‘Buster’ were used for final refinement. The final model contains 335 and 333 amino acids over 442, in molecules A and B, respectively, two FAD, three sulphate and 128 water molecules. Data collection and refinement statistics are reported in Table 2. Structural figures were prepared with PyMOL (http://www.pymol.org).

Accession number

The atomic coordinates of human renalase isoform 1 have been deposited in the RCSB Protein Data Bank with the accession code **3QJ4**.

References

1. Xu, J., Li, G., Wang, P., Velazquez, H., Yao, X., Li, Y., Wu, Y., Peixoto, A., Crowley, S. & Desir, G. V. (2005) Renalase is a novel, soluble monoamine oxidase that regulates cardiac function and blood pressure. J. Clin. Invest. 115, 1275-1280.
2. Desir, G. V. (2009) Regulation of blood pressure and cardiovascular function by renalase. Kidney Int. 76, 366-370.
3. Hennebry, S. C., Eikelis, N., Socratous, F., Desir, G. V., Lambert, G. & Schlaich, M. (2010) Renalase, a novel soluble FAD-dependent protein, is synthesized in the brain and peripheral nerves. Mol. Psychiatry 15, 234-236.
4. Desir, G. V. (2011) Role of renalase in the regulation of blood pressure and the renal dopamine system. Curr. Opin. Nephrol. Hypertens. 20, 31-36.
5. Desir, G. V. (2011) Novel insights into the physiology of renalase and its role in hypertension and heart disease. Pediatr Nephrol. [Epub ahead of print] PMID: 21424526.
6. Wu, Y., Xu, J., Velazquez, H., Wang, P., Li, G., Liu, D., Sampaio-Maia, B., Quelhas-Santos, J., Russell, K., Russell, R., Flavell, R. A., Pestana, M., Giordano, F. & Desir, G. V. (2010) Renalase deficiency aggravates ischemic myocardial damage. Kidney Int. 79, 853-860.
7. Zhao, Q., Fan, Z., He, J., Chen, S., Li, H., Zhang, P., Wang, L., Hu, D., Huang, J., Qiang, B., Gu, D. (2007) Renalase gene is a novel susceptibility gene for essential hypertension: a two-stage association study in northern Han Chinese population. J. Mol. Med. 85, 877-885.
8. Farzaneh-Far, R., Desir, G. V., Na, B., Schiller, N. B. & Whooley, M. A. (2010) A functional polymorphism in renalase (Glu37Asp) is associated with cardiac hypertrophy, dysfunction, and ischemia: data from the heart and soul study. PLoS ONE 5, e13496.

9. Weinman, E. J., Biswas, R., Steplock, D., Wang, P., Lau, Y. S., Desir, G. V. & Shenolikar, S. (2011) Increased renal dopamine and the acute renal adaptation to a high phosphate diet. Am. J. Physiol. Renal. Physiol. 300, F1123-F1129.
10. Gu, R., Lu, W., Xie, J., Bai, J. & Xu, B. (2011) Renalase deficiency in heart failure model of rats - a potential mechanism underlying circulating norepinephrine accumulation. PLoS ONE 6, e14633.
11. Wang, J., Qi, S., Cheng, W., Li, L., Wang, F., Li, Y. Z. & Zhang, S. P. (2008) Identification, expression and tissue distribution of a renalase homologue from mouse. Mol. Biol. Rep. 35, 613-620.
12. Li, G., Xu, J., Wang, P., Velazquez, H., Li, Y., Wu, Y. & Desir, G. V. (2008) Catecholamines regulate the activity, secretion, and synthesis of renalase. Circulation 117, 1277-1282.
13. Boomsma, F. & Tipton, K. F. (2007) Renalase, a catecholamine-metabolising enzyme? J. Neural Transm. 114, 775-776.
14. Medvedev, A. E., Veselovsky, A. V. & Fedchenko, V. I. (2010) Renalase, a new secretory enzyme responsible for selective degradation of catecholamines: achievements and unsolved problems. Biochemistry (Mosc) 75, 951-958.
15. Pandini, V., Ciriello, F., Tedeschi, G., Rossoni, G., Zanetti, G. & Aliverti, A. (2010) Synthesis of human renalase1 in *Escherichia coli* and its purification as a FAD-containing holoprotein. Protein Expr. Purif. 72, 244-253.
16. Massey, V. (1995) Introduction: flavoprotein structure and mechanism. FASEB J. 9, 473-475.
17. Massey, V. (2000) The chemical and biological versatility of riboflavin. Biochem. Soc. Trans. 28, 283-296.

18. Hynson, R. M., Kelly, S. M., Price, N. C. & Ramsay, R. R. (2004) Conformational changes in monoamine oxidase A in response to ligand binding or reduction. Biochim. Biophys. Acta 1672, 60-66.

19. Sablin, S. O., Yankovskaya, V., Bernard, S., Cronin, C. N. & Singer, T. P. (1998) Isolation and characterization of an evolutionary precursor of human monoamine oxidases A and B. Eur. J. Biochem. 253, 270-279.

20. Massey, V., Müller, F., Feldberg, R., Schuman, M., Sullivan, P. A., Howell, L. G., Mayhew, S. G., Matthews, R. G. & Foust, G. P. (1969) The reactivity of flavoproteins with sulfite. Possible relevance to the problem of oxygen reactivity. J. Biol. Chem. 244, 3999-4006.

21. Li, M., Hubálek, F., Newton-Vinson, P. & Edmondson, D. E. (2002) High-level expression of human liver monoamine oxidase A in *Pichia pastoris*: comparison with the enzyme expressed in *Saccharomyces cerevisiae*. Protein Expr. Purif. 24, 152-162.

22. Dym, O. & Eisenberg, D. (2001) Sequence-structure analysis of FAD-containing proteins. Protein Sci. 10, 1712-1728.

23. Fraaije, M. W. & Mattevi, A. (2000) Flavoenzymes: diverse catalysts with recurrent features. Trends Biochem. Sci. 25, 126-132.

24. Fitzpatrick, P. F. (2010) Oxidation of amines by flavoproteins. Arch. Biochem. Biophys. 493, 13-25.

25. De Colibus, L., Li, M., Binda, C., Lustig, A., Edmondson, D. E. & Mattevi, A. (2005) Three-dimensional structure of human monoamine oxidase A (MAO A): relation to the structures of rat MAO A and human MAO B. Proc. Natl. Acad. Sci. USA 102, 12684-12689.

26. Binda, C., Mattevi, A. & Edmondson, D. E. (2002) Structure-function relationships in flavoenzyme-dependent amine oxidations: a comparison of polyamine oxidase and monoamine oxidase. J. Biol. Chem. 277, 23973-23976.
27. Ballou, D. B., Entsch, B. & Cole, L. J. (2005) Dynamics involved in catalysis by single-component and two-component flavin-dependent aromatic hydroxylases. Biochem. Biophys. Res. Comm. 338, 590-598.
28. Wang, J., Ortiz-Maldonado, M., Entsch, B., Massey, V., Ballou, D. B. & Gatti, D. L. (2002) Protein and ligand dynamics in 4-hydroxybenzoate hydroxylase. Proc. Natl. Acad. Sci. USA 99, 608-613.
29. Sevrioukova, I. F. (2011) Apoptotosis-Inducing Factor: Structure, Function, and Redox Regulation. Antioxid. Redox Signal. 14, 2545-2579.
30. Massey, V. & Hemmerich, P. (1977) A photochemical procedure for reduction of oxidation-reduction proteins employing deazariboflavin as catalyst. J. Biol. Chem. 252, 5612-5614.
31. Milani, M., Balconi, E., Aliverti, A., Mastrangelo, E., Seeber, F., Bolognesi, M. & Zanetti, G. (2007) Ferredoxin-$NADP^+$ reductase from *Plasmodium falciparum* undergoes $NADP^+$-dependent dimerization and inactivation: functional and crystallographic analysis. J. Mol. Biol. 367, 501-513.
32. Vagin, A. & Teplyakov, A. (1997) MOLREP: an automated program for molecular replacement. J. Appl. Crystallogr. 30, 1022-1025.
33. Murshudov, G. N., Vagin, A. A. & Dodson, E. J. (1997) Refinement of Macromolecular Structures by the Maximum-Likelihood Method. Acta Crystallogr. D53, 240-255.
34. Emsley, P., Lohkamp, B., Scott, W. & Cowtan, K. (2010) Features and Development of Coot. Acta Crystallogr. D Biol. Crystallogr. 66, 486-501.

35. Cowtan, K. (2010) Recent developments in classical density modification. Acta Crystallogr. D Biol. Crystallogr. 66, 470-478.

Figure captions

Figure 1. Anaerobic photoreduction of renalase at different pH values. Progress of protein-bound FAD reduction as recorded on ca. 18 μM renalase in 10 mM phosphate-NaOH/10 mM pyrophosphate-NaOH, pH 6.5. The different traces represent the spectra recorded before (solid thin line) and as after each successive illumination periods (different line styles), until full reduction was obtained (solid thick line). The inset shows the maximal intensity reached at 600 nm in titrations carried out at different pH values. The interpolating line corresponds to the theoretical curve for the protonation of a single group with pK_a of 7.0 ± 0.3.

Figure 2. Titration of renalase with SO_3^{2-} anion. Spectra of renalase in the visible region recorded before (solid line) and after successive additions of $NaSO_3$ (0.5, 1.0, 2.0, 3.9, 8.8, 18, 37 mM final concentration) showing the progressive bleaching of bound FAD. The inset the reports the progress of FAD-sulfite adduct formation measured as the ratio between the A_{457} measured in the presence of increasing $NaSO_3$ concentrations and its initial value. The curve represents the theoretical equation for a 1:1 stoichiometry, whose fitting to the experimental data yielded a K_d of 1.8 ± 0.2 mM.

Figure 3. Catalytic activity of renalase on NADH and NADPH. Steady-state rate of the NADH- and NADPH-INT reductase reactions catalyzed by renalase, as monitored at 37 °C in 50 mM Tris-HCl, pH 7.2, are plotted as a function of reductant concentration.

Figure 4. Interaction of renalase with $NADP^+$, NAD^+, and 2'-P-AMP. Approximately 20 μM renalase was titrated with either $NADP^+$, NAD^+, or 2'-P-AMP at 25 °C in 50 mM Tris-

HCl, pH 7.4. Difference spectra extrapolated for ligand saturating conditions of the complexes of renalase with $NADP^+$ (solid line), NAD^+ (dashed line) and 2'-P-AMP (dotted line) are shown as extinction coefficient. In the inset the progress of the fractional amount of complexed protein is plotted as a function of $NADP^+$ (filled circles), NAD^+ (empty circles), or 2'-P-AMP (triangles) concentration. The curves represent the theoretical equation for a 1:1 stoichiometry, whose fitting to data yielded K_d of values of 1.6 ± 0.1 mM, 2.2 ± 0.1 mM, and 1.2 ± 0.3 mM, respectively.

Figure 5. Amino acid sequence and three-dimensional structure of human renalase.

(**A)** Multiple alignment of human renalase with orthologs from different organisms 110671808, *Mus musculus* (73% identity); 50540280, *Danio rerio* (60% identity); 193575653, *Acyrthosiphon pisum* (34% identity); 307154671, *Cyanothece* sp. (28% identity). Partially conserved residues are boxed, with invariant residues highlighted in red. Secondary structure elements are indicated above the renalase sequence.

(B) Renalase overall three-dimensional structure with secondary structure elements as highlighted in panel A. The FAD binding domain in shown red, the substrate-binding domain in blue, and the 62-108 subdomain in green.

Figure 6. Protein-FAD interactions and active-site cavity of renalase.

(A) The overlay of the three-dimensional structure of renalase to those of its most similar homologs is displayed on the left. The renalase molecule is shown as a green ribbon, with the FAD prosthetic group displayed as a wireframe in CPK colors. The Cα traces of *Exiguobacterium* sp. protoporphyrinogen oxidase (PDB ID: **3LOV**, blue color, rmsds 2.7 Å for 286 Cα), *Rhodococcus opacus* L-amino acid oxidase (PDB ID: **2JB2**, brown color, rmsds 2.5 Å for 292 Cα), and *H. sapiens* monoamine oxidase (PDB ID: **2BXR**, red color, rmsds 3.0

Å for 283 Cα) are also shown to highlight location of the third domain that is not present in renalase. The molecular surface of renalase, colored according to its potential (rotated by 90° respect to panel A), is displayed on the right. The entry of the active-site cavity, showing the pyrimidine side of the isoalloxazine ring of FAD, is clearly visible.

(B) Stereo view of the proposed renalase active-site region, showing FAD, the residues exchanging hydrogen bonds with FAD (green carbon atoms), the main residues lining the cavity above the isoalloxazine ring (blue carbon atoms), and the ordered sulphate ion bound at the border of the active-site cavity.

Tables

Table 1. Kinetic parameters of renalase for the NADH- and NADPH-dependent INT reductase reactions.[a]

Cosubstrate	k_{cat} (min^{-1})	K_m (μM)	k_{cat}/K_m ($min^{-1}\mu M^{-1}$)
NADH	0.14	18	$7.8\times10^{-3} \pm 1.2\times10^{-3}$
NADPH	0.26	175	$1.5\times10^{-3} \pm 1.4\times10^{-4}$

[a]INT-diaphorase activities of renalase were assayed at 37 °C in the presence of a fixed concentration of 100 μM INT.

Table 2. Crystallographic data collection and structure refinement statistics.

Data Collection Statistics	
Space group	P21
Unit-cell parameters (Å)	a=53.8 Å, b=86.6 Å, c=93.2 Å, α=γ= 90°, β= 95.3°
Resolution (Å)	48.4 - 2.5
Mosaicity (°)	1.0
№ of unique reflections	25,082 (3,770)
Completeness (%)	84.7 (87.5)
Redundancy	1.8 (1.8)
Rmerge † (%)	8.8 (49.5)
Average I/σ (I)	5.8 (1.9)
Refinement Statistics	
R factor ‡ (%)	21.7
Rfree § (%)	26.0
r.m.s. bond lengths (Å)	0.008
r.m.s. bond angles (°)	1.14
Ramachandran Plot	
Residues in most favoured regions (%)	89.3%
Residues in additionally allowed regions (%)	10.0%

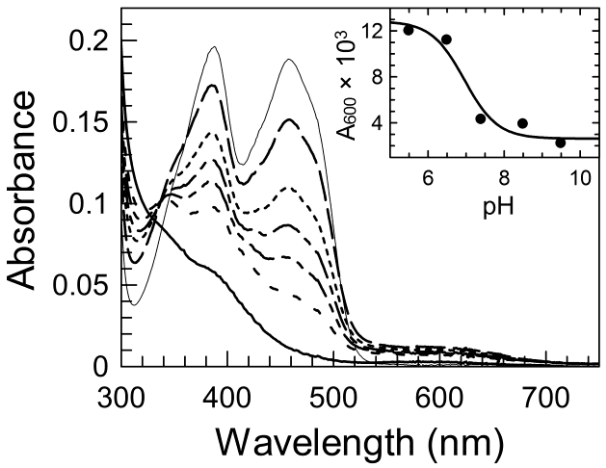
Absorbance
0.2
0.15
0.1
0.05
0
300
400
500
600
700
Wavelength (nm)
A600 × 10^3
12
8
4
6
8
10
pH

Fig. 1

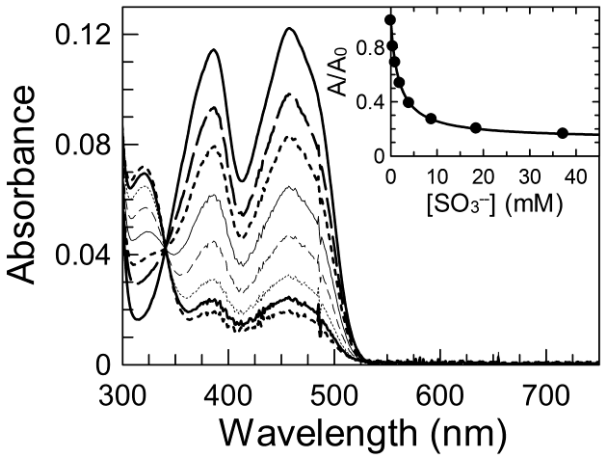
Absorbance
0.12
0.08
0.04
0
300
400
500
600
700
Wavelength (nm)
A/A0
0.8
0.4
0
0
10
20
30
40
[SO3−] (mM)

Fig. 2

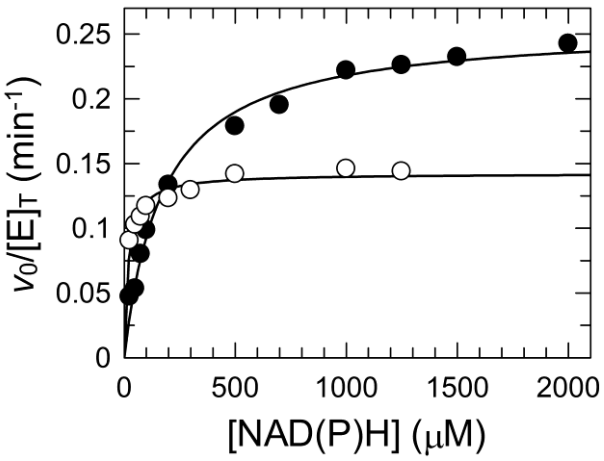

Fig. 3

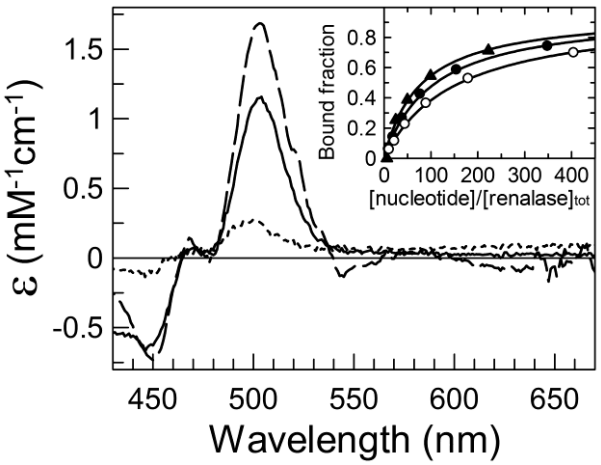
ε (mM-1cm-1)
1.5
1
0.5
0
-0.5
450
500
550
600
650
Wavelength (nm)
Bound fraction
0.8
0.6
0.4
0.2
0
0
100
200
300
400
[nucleotide]/[renalase]tot

Fig. 4

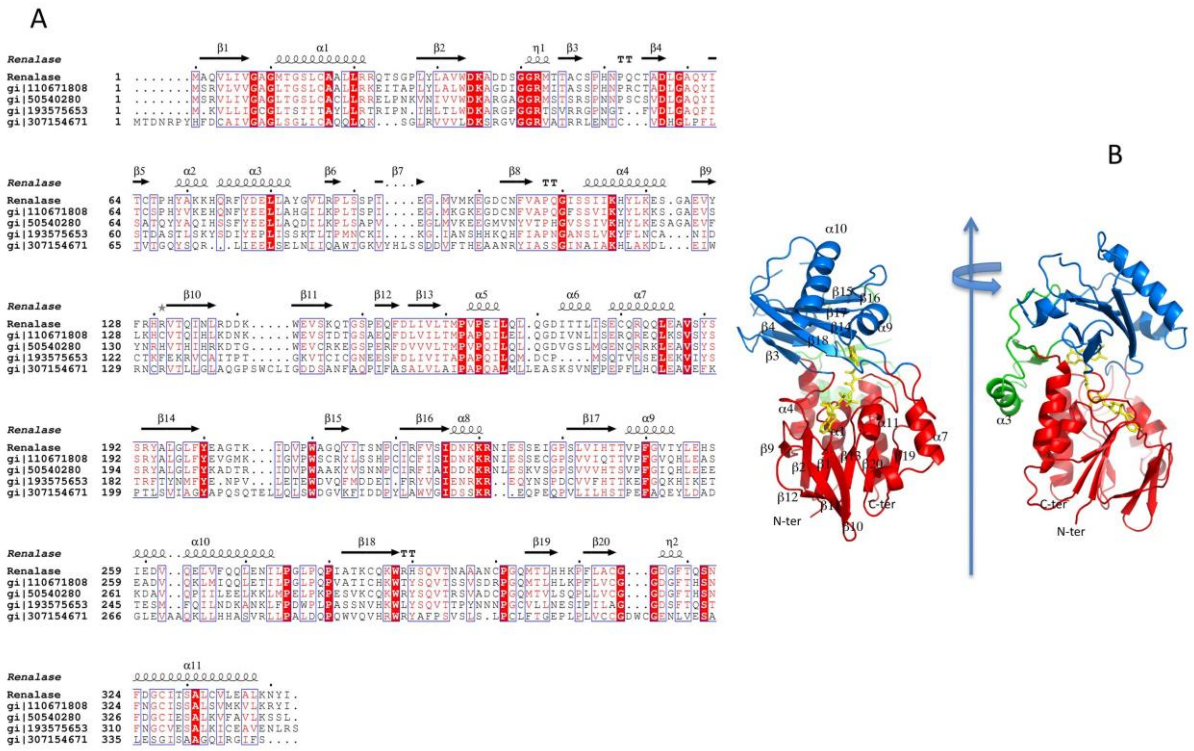
A
B
Renalase
gi|110671808
gi|50540280
gi|193575653
gi|307154671
N-ter
C-ter

Fig. 5

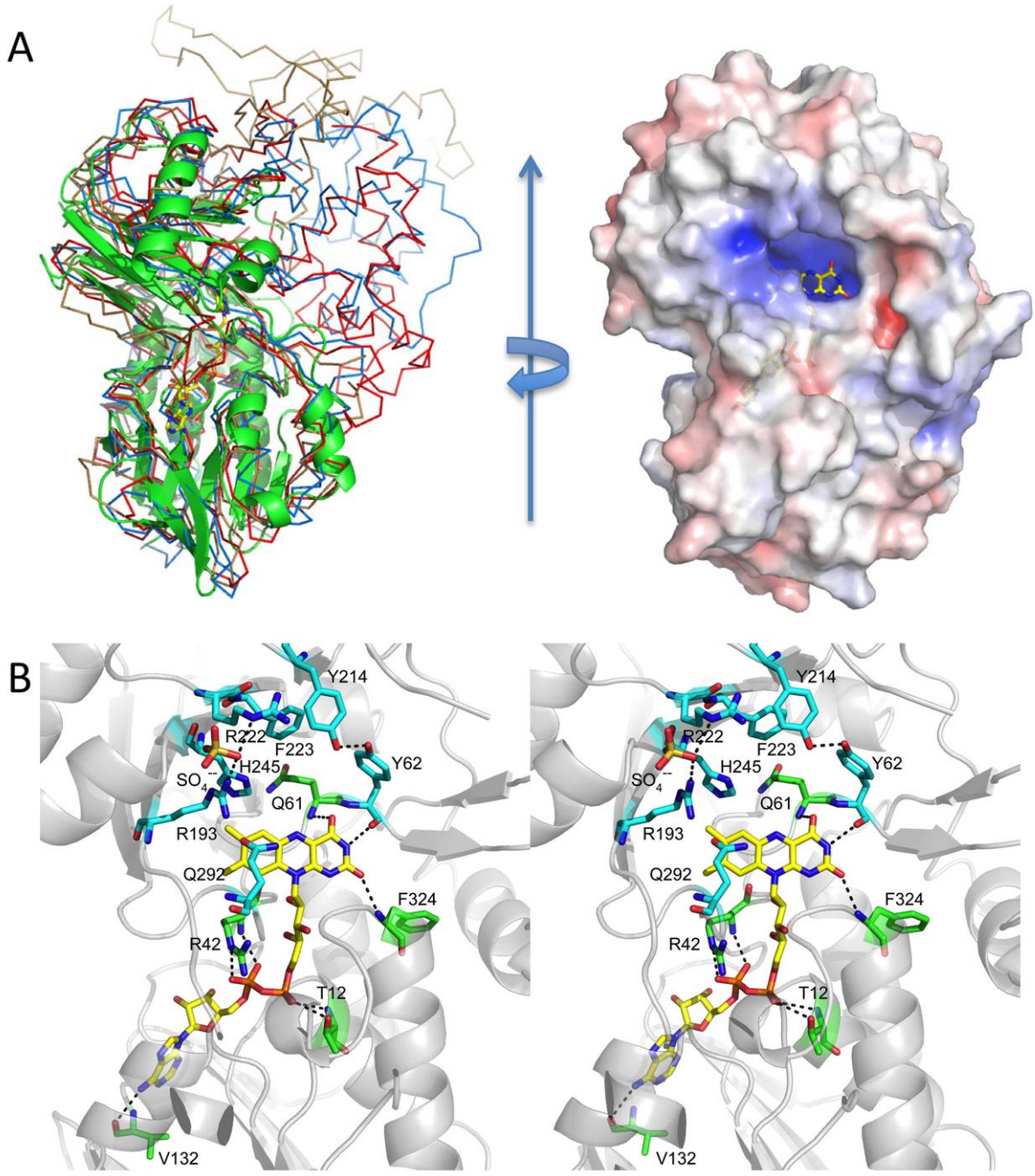

Fig. 6